



# Effect of TiO<sub>2</sub> percentage on the hydrogen-based direct reducibility of high-grade pellets

Behzad Sadeghi<sup>a,b,\*</sup>, Pasquale Cavaliere<sup>b,c,\*</sup>, Mutlucan Bayat<sup>b</sup>, Marieh Aminaei<sup>b</sup>,  
Niloofar Ebrahimzadeh Esfahani<sup>d,e</sup>, Aleksandra Laska<sup>f</sup>, Damian Koszelow<sup>g</sup>,  
Natalia Ramos Goncalves<sup>b</sup>

<sup>a</sup> Erich Schmid Institute of Materials Science, Austrian Academy of Sciences, Jahnstraße 12, A-8700 Leoben, Austria

<sup>b</sup> Department of Innovation Engineering, University of Salento, Via per Arnesano, 73100 Lecce, Italy

<sup>c</sup> Process Metallurgy Research Unit, Faculty of Technology, University of Oulu, 90570 Oulu, Finland

<sup>d</sup> Faculty of Electrical Engineering and Information, Slovak University of Technology, Ilkovicova 3, 81219 Bratislava, Slovakia

<sup>e</sup> Omnis Research Group, Department of Mathematics and Physics University of Salento, CNR-Institute of Nanotechnology, INFN Sezione di Lecce, Via per Monteroni, 73100 Lecce, Italy

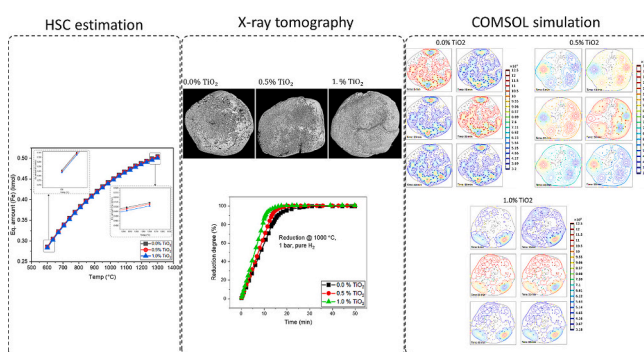
<sup>f</sup> Faculty of Mechanical Engineering and Ship Technology, Gdansk University of Technology, Narutowicza 11/12, 80-233 Gdansk, Poland

<sup>g</sup> Advanced Materials Centre, Faculty of Electronics, Telecommunications and Informatics, Gdansk University of Technology, 80-233 Gdansk, Poland

## HIGHLIGHTS

- TiO<sub>2</sub> below 0.5 % increases the reducibility of pellets by improving the structure.
- A high TiO<sub>2</sub> content reduces porosity and slows down reduction rates.
- Higher hydrogen pressure offsets the negative effects of TiO<sub>2</sub>.
- Study aligns theoretical predictions with the actual reduction behavior.

## GRAPHICAL ABSTRACT



## ARTICLE INFO

### Keywords:

Hydrogen-based direct reduction  
TiO<sub>2</sub>  
Reducibility  
High-grade pellet  
iron oxide

## ABSTRACT

The steel industry relies heavily on the direct reduction of iron ore pellets, which is a more environmentally friendly alternative to traditional blast furnaces, by reducing CO<sub>2</sub> emissions. This study investigated the effects of different TiO<sub>2</sub> contents on the reducibility of high-grade iron ore pellets using hydrogen (H<sub>2</sub>). The research employed HSC chemistry, COMSOL Multiphysics, and X-ray tomography to analyse the thermodynamics and kinetics of hematite reduction. The results indicate that TiO<sub>2</sub> significantly affects reducibility; pellets with less than 0.5 % TiO<sub>2</sub> show improved reducibility due to favorable microstructural changes, while higher TiO<sub>2</sub> content reduces porosity and slows down reduction rates. However, increasing the H<sub>2</sub> pressure to 8 bar mitigated the detrimental effects of the high TiO<sub>2</sub> content and improved the porosity and reduction kinetics. These results

\* Corresponding authors at: Department of Innovation Engineering, University of Salento, Via per Arnesano, 73100 Lecce, Italy.

E-mail addresses: [behzad.Sadeghi@oaw.ac.at](mailto:behzad.Sadeghi@oaw.ac.at) (B. Sadeghi), [pasquale.cavaliere@unisalento.it](mailto:pasquale.cavaliere@unisalento.it) (P. Cavaliere).

<https://doi.org/10.1016/j.powtec.2025.120813>

Received 5 July 2024; Received in revised form 8 February 2025; Accepted 13 February 2025

Available online 15 February 2025

0032-5910/© 2025 The Authors. Published by Elsevier B.V. This is an open access article under the CC BY license (<http://creativecommons.org/licenses/by/4.0/>).

support the theoretical predictions, provide guidelines for optimizing pellet formulations, and emphasize the importance of controlling the TiO<sub>2</sub> content and operating conditions for efficient reduction processes.

## 1. Introduction

The steel industry is responsible for approximately 30 % of global industrial CO<sub>2</sub> emissions and produces 1.9 billion tons of steel annually, mainly using the blast furnace-to-oxygen converter process (BF-BOF). For this reason, decarbonization is urgently needed to ensure climate stability over the next two decades [1–3]. Timely reduction of CO<sub>2</sub> emissions is crucial because of their long-lasting atmospheric impact [4]. Replacing carbon with green H<sub>2</sub> produced from renewable energy sources as a reducing agent is a promising route for cleaner and more sustainable iron production [5]. This switch has the advantage of producing water as a by-product instead of CO<sub>2</sub> [6–8], which contributes to environmentally friendly industrial practices.

The direct reduction of iron ore pellets is a pivotal process in the steelmaking industry, offering an environmentally friendly alternative to traditional blast furnace methods [1,9]. The direct reduction process converts centimeter-sized polycrystalline sintered oxide pellets, known as DRI, into sponge iron by removing the oxygen. This is usually performed using reducing agents such as H<sub>2</sub> (HyDR) or CO at high temperatures, producing 93–98 % metallized sponge iron. The efficiency and effectiveness of this process are significantly influenced by the material properties of the pellets, including their mineralogical composition and the presence of specific additives. One such additive, titanium dioxide (TiO<sub>2</sub>), has garnered attention because of its potential impact on the reducibility of iron-ore pellets.

Research has shown that the presence of TiO<sub>2</sub> in iron ore pellets can affect their reduction behavior and final properties [10]. These studies have highlighted the complex relationship between TiO<sub>2</sub> and the direct reducibility of iron ore, with conflicting findings regarding the effects of TiO<sub>2</sub> levels on the reduction efficiency [11,12]. TiO<sub>2</sub> is known to interact with other components of the pellets during the reduction process, potentially leading to variations in the porosity, phase transformations, oxidation rate, reduction degree, and mechanical strength of the reduced pellets. The interaction of TiO<sub>2</sub> with other pellet components during reduction plays a crucial role in determining its final properties. Different studies have highlighted the complex relationship between TiO<sub>2</sub> content and the physical characteristics of pellets, emphasizing the need for a comprehensive understanding of these interactions for optimized pellet production. Ju et al. [13] showed that in the presence of TiO<sub>2</sub> as the basicity increases the porosity increases first and then decreases while the compressive strength is opposite to porosity to decrease first and then increases. Yang et al. [14] reported that as the TiO<sub>2</sub> content increased, the magnetite phase increased, while the hematite phases decreased. They also demonstrated that the lower the TiO<sub>2</sub> content, the better is the quality of the sintering process. According to documented A small amount of TiO<sub>2</sub> can enhance reducibility by creating beneficial microstructural changes [11], while others have reported a decrease in reduction efficiency with higher TiO<sub>2</sub> content due to the formation of stable titaniferous phases that are difficult to reduce [12,15]. Some studies have indicated that a higher TiO<sub>2</sub> content can hinder the reduction process. However, other studies report more nuanced effects, where the effect of TiO<sub>2</sub> depends on the mineralogical composition of the ore and the specific reduction conditions. Therefore, it can be concluded that there is still no comprehensive understanding of the exact mechanisms by which TiO<sub>2</sub> affects the direct reducibility of high-grade iron ore pellets, a common feedstock for direct reduction processes.

Despite extensive research on factors influencing the direct reducibility of DRI, including sintering and processing parameters, as well as raw material composition, there are still significant knowledge gaps regarding the specific influence of TiO<sub>2</sub> content on the reducibility of

high-quality iron oxide pellets. Existing studies mainly focus on the main parameters such as the CaO/SiO<sub>2</sub> ratio (basicity), while little attention has been paid to the role of minor components such as TiO<sub>2</sub> and their comprehensive effects on the reduction behavior. Some studies suggest that TiO<sub>2</sub> can induce microstructural changes that are beneficial for reducibility when present in small amounts [11,12], while other studies indicate that a higher TiO<sub>2</sub> content can hinder the reduction process owing to the formation of stable, difficult-to-reduce titanium-containing phases [13]. However, these results are often contradictory and lack depth regarding the mechanisms underlying observed effects, leading to conflicting interpretations.

This study uniquely contributes to filling this research gap by systematically analyzing how different proportions of TiO<sub>2</sub> affect the reducibility of high-grade iron ore pellets during hydrogen-based direct reduction. Through the use of a combination of HSC chemistry modeling, COMSOL Multiphysics simulations, and X-ray tomography, this study provides a comprehensive understanding of the thermodynamic and kinetic behavior associated with TiO<sub>2</sub> content. In particular, the study shows that a lower TiO<sub>2</sub> content (<0.5 %) improves reducibility owing to favorable microstructural transformations, while higher contents negatively affect porosity and reduction kinetics. Furthermore, this study shows that increasing the hydrogen pressure can mitigate the detrimental effects of higher TiO<sub>2</sub> concentrations, an aspect that has not been extensively studied in the literature. This integrated approach, combining theoretical predictions with practical experiments, sets a precedent for the optimization of pellet formulations and reduction parameters to improve the efficiency and sustainability of hydrogen-based iron production processes.

## 2. Experimental procedure

A series of reduction experiments were carried out to investigate the effects of varying the TiO<sub>2</sub> content on the reducibility of the iron ore pellets. The iron ore pellets used in this study were characterized to evaluate the distribution and morphology of TiO<sub>2</sub> prior to reduction. TiO<sub>2</sub> was predominantly dispersed in the pellet matrix as fine particles. Microscopic observations and elemental analyses showed that these particles were uniformly distributed and typically ranged in size from 1 to 5 μm. The fine dispersion of TiO<sub>2</sub> was observed to improve matrix uniformity and maintain structural integrity prior to reduction. Key methods included preparing pellets with controlled TiO<sub>2</sub> content, performing thermodynamic modeling using HSC Chemistry software, and conducting reduction experiments in a custom reactor at 950–1000 °C with high-purity hydrogen (99.99 %). The individual steps of the optimized methodology are provided below.

The iron ore pellets were supplied by VALE (Brazil), where the production process of the pellets is described in detail in [16], and the compositions are shown in Table 1. The average chemical composition and physical properties of the pellets were verified before testing.

Thermodynamic simulations were performed using HSC Chemistry 6 to determine the equilibrium compositions of the reactions involving Fe<sub>2</sub>O<sub>3</sub> and hydrogen, following the reduction sequence of Fe<sub>2</sub>O<sub>3</sub> to Fe. The indicated reactions are listed below.

**Table 1**  
Specifications of the analysed pellets, including average size and density.

Pellet	Average size, cm	Density, g/cm <sup>3</sup>
small	1.14	2.6
medium	1.36	3.5
big	1.72	3.4



The initial amounts of each oxide species were entered into the software, considering their percentage in each pellet and their total moles based on their molar mass. The equilibrium compositions of all the species involved, including oxides, elemental metals, water vapor, and all other relevant compounds, were recorded. All oxides and their reduced metals were in the solid phase, whereas  $\text{H}_2$ ,  $\text{H}_2\text{O}$ , and gaseous forms of the metals were introduced in the gas phase. Three different compositions with different proportions of  $\text{TiO}_2$ , slightly different proportions of  $\text{SiO}_2$  and  $\text{CaO}$ , and the same proportions of  $\text{Al}_2\text{O}_3$  and  $\text{Fe}_2\text{O}_3$  were considered, as shown in Table 2.

At the starting point, the initial concentrations of the iron oxide derivatives ( $\text{Fe}_3\text{O}_4$ ,  $\text{FeO}$ , and  $\text{Fe}$ ), with the exception of  $\text{Fe}_2\text{O}_3$ , were considered to be zero to determine the composition of the system based on the reactions and specified conditions. The weight of the sample used to calculate the number of moles to be introduced was 100 kg. The molar ratio of  $\text{H}_2$  to the sum of moles of the starting oxides was assumed to be 3:1. The temperature and pressure were assumed as 600–1300 °C and 1 bar, respectively.

Pure hydrogen was used at pressures of 1 and 8 bar to isolate its influence on reducibility and microstructural changes. A flow rate of 0.5 l/min, chosen based on initial testing and literature [5,17], ensures thorough reduction and is consistent with industrial practice for applicability. Three tests were performed for each condition to ensure reproducibility of the results. The microstructures before and after reduction were examined using X-ray microtomography to observe changes in porosity [16,18]. ImageJ and COMSOL Multiphysics v.6.2 were used to analyse the pore structure and model the gas-solid interaction.

The FIJI/ImageJ software was used to obtain the pore structure together with the solid-gas interface. The simulations were performed using commercial COMSOL Multiphysics v.6.2. Regression analyses were performed using commercial Minitab statistical software, and the details are provided in the Supplementary materials. The exact values of the assumptions used in the COMSOL simulations are listed in Table 3. The following assumptions were made during the simulations:

- $\text{H}_2$  is considered to be an ideal compressible gas.
- The reactive bed filled with pellets was completely isolated.
- The reduction process required 50 min to complete.
- The initial ambient temperature is 20 °C.
- The initial velocity of gas inside the bed is considered as 5 m/s.
- For the pore-wall interaction, the Knudsen equation was used to calculate the wall diffusivity.
- For the velocity distribution and the convection, the Darcy's law is employed.
- The surface chemical reactions are considered reversible.

To ensure the reproducibility and validity of the experimental results, a rigorous statistical analysis was performed. The standard deviation was calculated for each set of measurements to assess data consistency. Regression analysis was used to evaluate the relationship between the  $\text{TiO}_2$  content and reduction kinetics, with statistical significance determined at a  $p$ -value of 0.05. Minitab statistical software

**Table 2**  
The pellet composition (wt%).

Pellet	$\text{Fe}_2\text{O}_3$	$\text{TiO}_2$	$\text{CaO}$	$\text{Al}_2\text{O}_3$	$\text{SiO}_2$	Basicity index
1	95.57	0	1.63	0.47	2.33	0.69
2	95.57	0.5	1.46	0.47	2.0	0.73
3	95.57	1	1.26	0.47	1.7	0.74

**Table 3**  
Assumptions adopted in COMSOL simulations.

Parameter	Independent
Operating temperature	1000 °C
$\text{H}_2$ Pressure	1 bar
Velocity of $\text{H}_2$	5 m/s
Minimum element size	0.0059 mm
Maximum element size	1.32 mm
Maximum element growth rate	1.3
Curvature factor	0.3

was used for data processing and validation. This approach enabled the identification of trends and verification of experimental repeatability, and ensured that the observed effects were statistically robust and reproducible.

### 3. Results and discussion

In direct reduction, oxides such as  $\text{CaO}$ ,  $\text{Al}_2\text{O}_3$ ,  $\text{TiO}_2$ , and  $\text{SiO}_2$  are usually present, which can influence the overall kinetics and thermodynamics of the reaction system. These oxides can act as catalysts, inhibitors or promoters and influence the efficiency and selectivity of iron oxide reduction. Understanding the thermodynamics of iron oxide reduction is crucial for optimizing production methods and increasing the efficiency of iron production. HSC chemistry software analyzes the thermodynamic properties of the reaction system and is a useful tool for studying and simulating the thermodynamics of the reactions. Therefore, HSC Chemistry software was used to study the thermodynamic aspects of the direct reduction of iron oxides in the presence of  $\text{H}_2$  gas. In addition, we considered the effects of non-ferrous oxides such as  $\text{TiO}_2$ ,  $\text{CaO}$ ,  $\text{Al}_2\text{O}_3$  and  $\text{SiO}_2$  on the overall reduction process. The reduction of  $\text{Fe}_2\text{O}_3$  to  $\text{Fe}$  involves hierarchical but complex chemical transformations, each of which is governed by thermodynamic and kinetic principles. First,  $\text{Fe}_2\text{O}_3$  reacts with  $\text{H}_2$  to form  $\text{Fe}_3\text{O}_4$ , followed by further reduction steps that produce  $\text{FeO}$ , and consequently, elemental  $\text{Fe}$ . Fig. 1 shows that the amount of  $\text{Fe}$  increased with increasing temperature and that all three pellets followed the same pattern. However, the 0.0 %  $\text{TiO}_2$  pellet produced a greater amount of  $\text{Fe}$  than the other two pellets (Fig. 1). Interestingly, the difference between the pellets increased as the temperature increased, indicating that the 0.0 %  $\text{TiO}_2$  pellet produced more  $\text{Fe}$ . It appears that more  $\text{TiO}_2$  leads to a lower  $\text{Fe}$  content.

The general tendency of  $\text{FeO}$  change increased as the temperature increased. At the beginning of the simulation, the  $\text{FeO}$  content in the 0.0

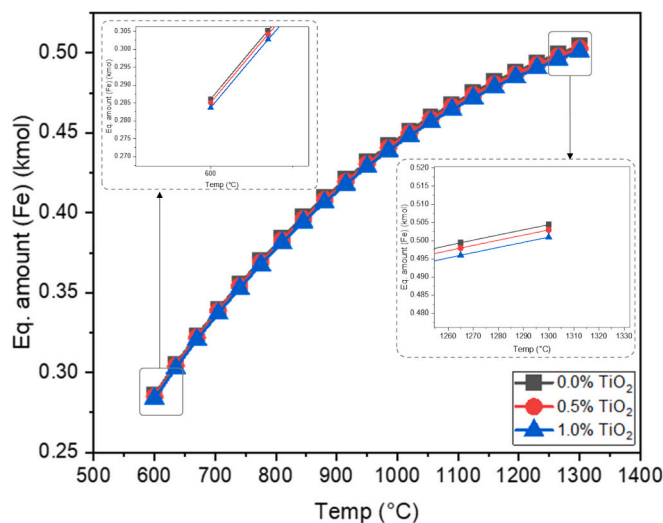


**Fig. 1.** Evolution of the thermodynamic equilibrium of Fe concentration for different pellets during HyDR as a function of temperature.

% TiO<sub>2</sub> pellet is higher, while the 1.0 % TiO<sub>2</sub> pellet contains more FeO until the end of the simulation when the temperature of 980 °C is reached. This could be due to the fact that more Fe is produced in pellet 0.0 % TiO<sub>2</sub> at higher temperatures. In addition, the amount of FeO produced appeared to be higher than that of Fe at all temperatures and pellets, suggesting that FeO may be the predominant product of the reduction process under these conditions. The difference between the amounts of Fe and FeO produced varied depending on the temperature and pellets, suggesting that the reduction process is influenced by factors such as temperature, composition, and reaction kinetics (Fig. 2).

Fig. 3 shows the equilibrium concentrations of Fe<sub>3</sub>O<sub>4</sub> and Fe<sub>2</sub>O<sub>3</sub> as a function of temperature for pellets with different TiO<sub>2</sub> contents during the HyDR process. Fig. 3 (a) shows a consistent decrease in the Fe<sub>3</sub>O<sub>4</sub> concentration with increasing temperature for all three pellet compositions (0.0, 0.5, and 1.0 % TiO<sub>2</sub>). This decrease indicates that higher temperatures favor further reduction of Fe<sub>3</sub>O<sub>4</sub> to Fe, which is consistent with the exothermic nature of the reduction reactions and the increased reaction rates at elevated temperatures. Remarkably, the plot shows no significant difference in the Fe<sub>3</sub>O<sub>4</sub> concentration between the different TiO<sub>2</sub> fractions, indicating that the TiO<sub>2</sub> concentration within the investigated temperature range has no significant effect on the Fe<sub>3</sub>O<sub>4</sub> reduction equilibrium. Fig. 3 (b) shows a similar trend for Fe<sub>2</sub>O<sub>3</sub>, where the Fe<sub>2</sub>O<sub>3</sub> concentration decreases steadily with increasing temperature. As expected, this was due to the reduction of Fe<sub>2</sub>O<sub>3</sub> to Fe<sub>3</sub>O<sub>4</sub>, which is a precursor step for the reduction to metallic Fe. Again, the lines for the different TiO<sub>2</sub> contents almost overlap, indicating that the TiO<sub>2</sub> content does not significantly change the Fe<sub>2</sub>O<sub>3</sub> reduction behavior under these conditions. The pellet with 1.0 % TiO<sub>2</sub> had the highest Fe<sub>3</sub>O<sub>4</sub> concentration at lower temperatures; however, as the temperature increased, the differences between the pellets decreased. This could indicate that TiO<sub>2</sub> influences the initial reduction stages but has less influence at higher temperatures, where reduction to metallic Fe dominates.

The reduction of iron oxides with H<sub>2</sub> gas produces water as a by-product of the reaction. Higher water production may indicate more efficient reduction reactions in which the reactants (for example, Fe<sub>2</sub>O<sub>3</sub>) are effectively converted into products (e.g. Fe). Conversely, a lower water production could indicate the formation of intermediate oxide phases (for example, FeO or Fe<sub>3</sub>O<sub>4</sub>), instead of the desired Fe product. However, it is important to consider other factors as well. The pellet with 0.0 % TiO<sub>2</sub> produced more water in all temperature ranges, followed by pellets with 0.5 % TiO<sub>2</sub> and pellets with 1.0 % TiO<sub>2</sub>. This indicates that TiO<sub>2</sub> is an obstacle to further reactions.

Fig. 5 shows the equilibrium composition of FeO as a percentage of

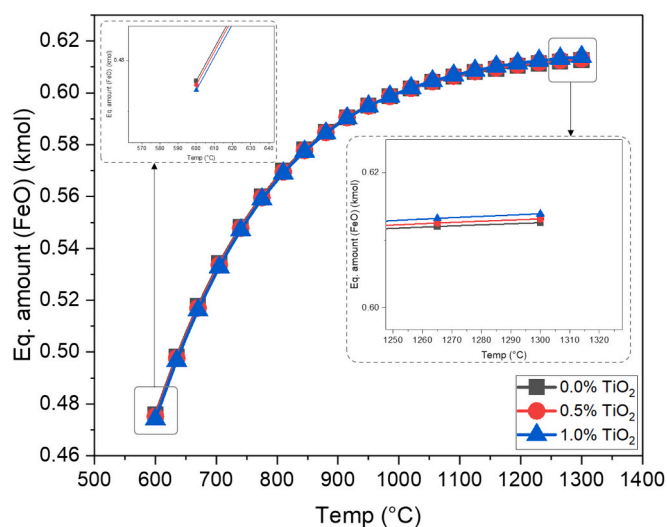


Fig. 2. Evolution of the thermodynamic equilibrium of FeO concentration for different pellets during HyDR as a function of temperature.

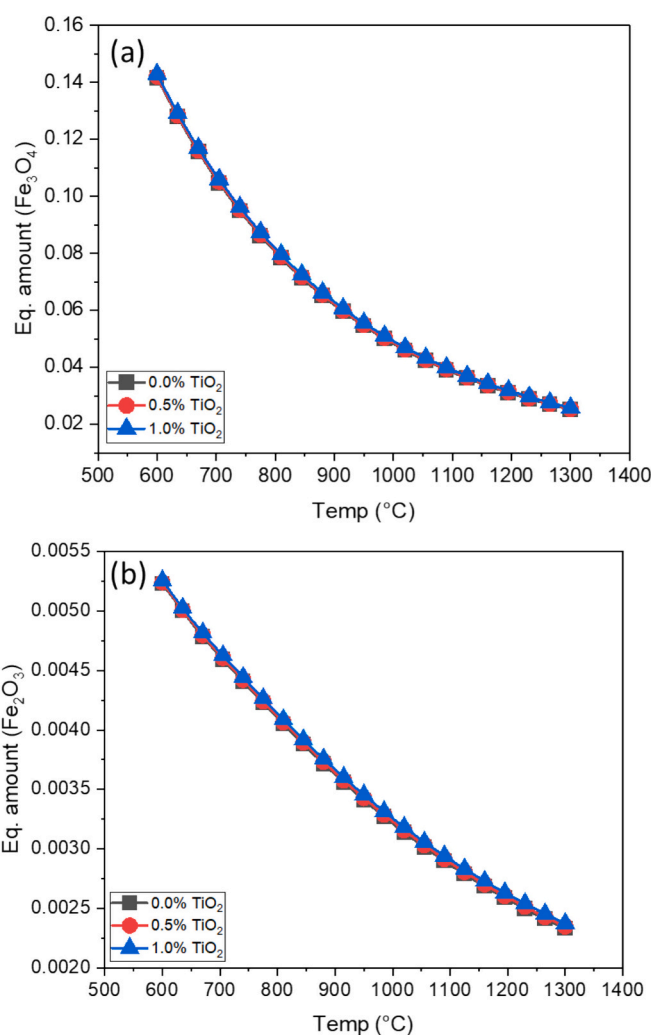


Fig. 3. Evolution of the thermodynamic equilibrium of Fe<sub>3</sub>O<sub>4</sub> and Fe<sub>2</sub>O<sub>3</sub> concentrations for different pellets during HyDR as a function of temperature. (a) Fe<sub>3</sub>O<sub>4</sub> and (b) Fe<sub>2</sub>O<sub>3</sub>.

total moles plotted against temperature for three different iron-oxide pellet samples during the HyDR process. The FeO content increased with temperature in all the samples, reaching a peak between 1000 and 1100 °C. This behavior is consistent with the general trend that the mole fraction of Fe increases with increasing temperature, indicating the progression of the reduction reaction, where higher temperatures promote the conversion of iron oxides to Fe. At lower temperatures, especially 600 °C, the FeO percentages of all samples were close to each other and showed no significant differences. This indicates that, at this stage of the reduction process, the TiO<sub>2</sub> content had no significant effect on the formation of FeO. As the temperature increased further, the equilibrium composition of FeO began to decrease in all the samples, indicating that FeO was further reduced to elemental Fe. The decrease in the FeO composition at higher temperatures indicates a shift in equilibrium conditions that favor the formation of metallic iron over the oxide. Notably, the sample with 1.0 % TiO<sub>2</sub> had the highest FeO composition over the entire temperature range, and the differences between the samples became more pronounced at higher temperatures. For example, there was a difference of 0.22 % at 600 °C and 0.39 % at 1300 °C between pellets 1 (0.0 % TiO<sub>2</sub>) and 3 (1.0 % TiO<sub>2</sub>). The presence of TiO<sub>2</sub> appears to affect the thermodynamics or kinetics of the reactions, possibly by influencing factors, such as the stability of FeO or the rate of its reduction to Fe. The fact that the pellet with a higher TiO<sub>2</sub> content had a higher FeO content suggests that TiO<sub>2</sub> could hinder the reduction

of FeO to Fe, either by physically hindering the reaction or by altering the chemical equilibrium. The consistent trends in Figure 1 Figure 2 Figure 5 illustrate the complex interplay between temperature, pellet composition and equilibrium states of the iron oxides during reduction. Therefore, it can be concluded that the TiO<sub>2</sub> content exerts a subtle influence on the kinetics and thermodynamics of these reactions.

The linear increase in enthalpy observed in Fig. 6 over the temperature range 600–1300 °C indicates an endothermic process in which the energy required for the reduction of iron oxides to metallic Fe is gradually absorbed from the environment. This steady increase in enthalpy, independent of the TiO<sub>2</sub> content, suggests that TiO<sub>2</sub> does not significantly affect the total energy absorbed in the system during the temperature interval studied. Furthermore, the lack of phase changes or reaction threshold anomalies in this range suggests that the pellets underwent a consistent reduction process without significant physico-chemical transformations that can be detected via enthalpy changes. This supports the earlier observations from Figs. 1 and 2 that Fe and FeO concentrations increase steadily with temperature, indicating a progressive and unhindered reduction sequence from Fe<sub>2</sub>O<sub>3</sub> to Fe<sub>3</sub>O<sub>4</sub>, then to FeO, and finally to metallic Fe, without any discernible interference from varying TiO<sub>2</sub> contents. This is consistent with the previous results published in [19–21].

Correlating these observations with Fig. 5 shows that FeO composition peaks and decreases at higher temperatures. The consistent energy uptake in Fig. 6 supports that temperature-controlled reduction primarily determines reaction kinetics, rather than TiO<sub>2</sub> content [22–25]. Slight differences in FeO composition at peak temperatures, more noticeable in pellets with higher TiO<sub>2</sub> content, could stem from factors unrelated to enthalpy changes. These factors may include physical properties like porosity and surface area, which can influence reduction kinetics.

Building on the thermodynamic insights gained from the HSC simulation, the results are now compared with experimental data and COMSOL Multiphysics simulation results. This analysis validates theoretical predictions with experimental observations and refines the understanding of the influence of TiO<sub>2</sub> on the reducibility of pellets. It examines the agreement between the measured reduction kinetics, the temperature-dependent behavior and the simulations.

Fig. 7 provides experimental data on the reduction kinetics of hematite pellets with varying TiO<sub>2</sub> content during HyDR at 1000 °C. The experimental data shown in Fig. 7 (a) and (b) confirm the reduction sequence timeline identified in our database and preliminary experimental results. As a matter of fact, the stages of reduction of Fe<sub>2</sub>O<sub>3</sub> to Fe<sub>3</sub>O<sub>4</sub>, Fe<sub>3</sub>O<sub>4</sub> to FeO and FeO to Fe correspond to specific time intervals of about 2–5 min, 5–30 min and 30–50 min, respectively, which is consistent with previous publication [29]. In addition, the reducibility naturally decreases the higher the TiO<sub>2</sub> content in the pellet. The HyDR process involves a hierarchy of phenomena, including transport phenomena and reaction kinetics, which govern the chemical reactions on different length and time scales. The observed changes in the reaction rate (expressed as mass loss per time) versus time curve can be attributed to these kinetic and thermodynamic differences [26–30]. At a high temperature, such as 1000 °C, the phases corresponding to the reduction of Fe<sub>2</sub>O<sub>3</sub> to Fe<sub>3</sub>O<sub>4</sub> and then to FeO and Fe may partially overlap, which is why the regions related to each phase are not clearly separated in Fig. 7 (b). The peak at the beginning indicates the fastest reaction rate, which is related to the reduction of Fe<sub>2</sub>O<sub>3</sub> to Fe<sub>3</sub>O<sub>4</sub>, which is known to occur rapidly. As the temperature is high and the H<sub>2</sub> atmosphere is conducive to reduction, this stage is quickly passed. This observation is consistent with the findings [11,29], according to which the rate and degree of reduction increase with increasing TiO<sub>2</sub> content. The subsequent slower but steady decrease in rate may reflect the reduction of Fe<sub>3</sub>O<sub>4</sub> to FeO and then to metallic Fe. The presence of TiO<sub>2</sub>, particularly in the 1.0 % TiO<sub>2</sub> sample, appears to slow the rate of reduction slightly, as indicated by a broader peak and a more gradual decline in rate compared to the 0.0 %

TiO<sub>2</sub> sample. The overall trend in Fig. 7, when correlated with the HSC simulation results, shows that while the TiO<sub>2</sub> content of up to 1.0 % does not significantly change the final extent of iron oxide reduction, it does affect the rate at which these reductions occur. This suggests that the TiO<sub>2</sub> content play a role in influencing the kinetics of the HyDR process. It influences the rate of H<sub>2</sub> diffusion or surface reactions without significantly altering the thermodynamic equilibrium of the system.

The structure of the pellets was analysed by X-ray tomography. The appearance of the 0.0 % TiO<sub>2</sub> pellet before and after direct H<sub>2</sub> reduction is shown in Fig. 8. The appearance of the pellets with higher TiO<sub>2</sub> content is shown in Fig. 2S in the supplementary material and is available as online material. All these figures show the structural changes in hematite pellets with different TiO<sub>2</sub> contents before and after the HyDR process at 1000 °C for 50 min. In the images after the reduction of Fig. 2S (0.5 % TiO<sub>2</sub>) and Fig. 2S (1.0 % TiO<sub>2</sub>), an increase in the heterogeneity of the grey scale can be seen compared to the images before the reduction. This is an indication of the chemical transformation caused by the reduction, with lighter areas within the pellets indicating a stronger reduction in the center. There are no significant differences in the internal structure between Figs. 2S due to the different TiO<sub>2</sub> content, indicating that a TiO<sub>2</sub> content of up to 1.0 % does not noticeably change the physical transformation of the pellets during HyDR. In Fig. 8, similar transformation trends can be seen in the structures after reduction, with increased porosity and fragmentation in the medium and small sized pellets due to the extensive reduction and the evolution of gasses.

A comparison of the 3D micrographic images for different TiO<sub>2</sub> contents shows that the structural changes after reduction do not differ significantly from the TiO<sub>2</sub> contents. The extensive changes in the grayscale distribution after HyDR treatment in all pellets indicate a high degree of reduction. The high degrees of reduction shown in Fig. 7 (a) are consistent with the significant structural changes observed in the post-reduction microtomographic images. Although Fig. 7 (b) shows a slight decrease in the rate of reduction for pellets with higher TiO<sub>2</sub> content, this is not clearly reflected in the microtomographic images, which show no clear differences in the extent of reduction as a function of TiO<sub>2</sub> content. This indicates that although the kinetics of the reduction process can be influenced by TiO<sub>2</sub>, the final extent of reduction within the experimental time frame is not significantly affected.

Per each pellet, 2D sections were selected in order to be able to analyse the porosity evolution. The evolution of porosity in different pellet sizes with different TiO<sub>2</sub> content before and after reduction, as shown in Fig. 9 (0.0 % TiO<sub>2</sub>), was analysed. The 2D sections of the other pellets with different dimension and with different TiO<sub>2</sub> content is

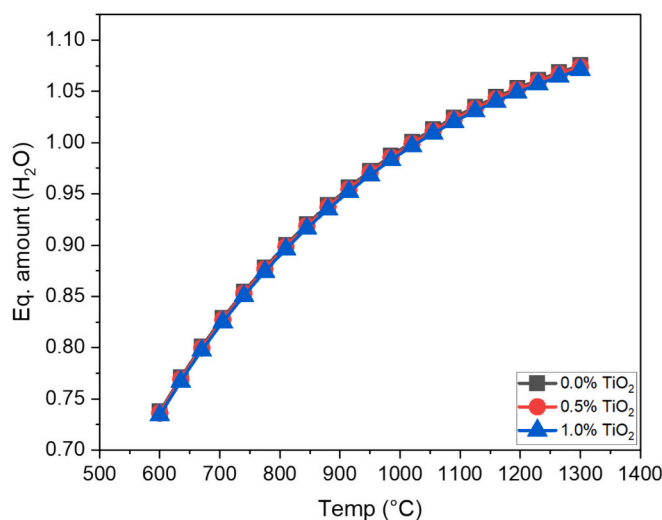


Fig. 4. Evolution of the thermodynamic equilibrium of H<sub>2</sub>O in different pellets as byproducts of reducing iron oxides with H<sub>2</sub> gas.

shown in Fig. 3S (0.5 % TiO<sub>2</sub>) and Fig. 4S (1.0 % TiO<sub>2</sub>) in Supplementary material and available as online material. It was found that the pellets of all sizes and TiO<sub>2</sub> contents had a uniform grey scale before reduction, indicating a homogeneous hematite structure. After reduction, an increase in porosity was observed across all sizes and TiO<sub>2</sub> contents. The increased porosity is indicated by lighter areas within the reduced pellets, probably caused by the evolution of gases such as water vapor and H<sub>2</sub> during the reduction of iron oxide to metallic iron. For small pellets (as shown in Fig. 9 (a), and Figs. 3S(a), and 4S(a)), the increase in porosity after reduction is noticeable, but less pronounced than for larger pellets. This indicates that the uniform distribution of heat and H<sub>2</sub>, which is favoured by the smaller size, leads to a more homogeneous reduction process throughout the pellet.

Medium sized pellets (as seen in Fig. 9 (b), and Figs. 3S(b), and 4S (b)) were found to have a greater increase in porosity after reduction compared to small pellets. The medium pellet size likely allows for a higher degree of reduction and gas evolution without the diffusion limitations observed with the largest pellets. The largest pellets (shown in Fig. 9 (c), and Figs. 3S(c), and 4S(c)) show the most significant changes in porosity, with the reduced pellets exhibiting extended bright areas. It can be concluded that the larger size of these pellets leads to more pronounced temperature and H<sub>2</sub> concentration gradients during the reduction process, resulting in non-uniform reduction and more variable porosity. As far as the influence of TiO<sub>2</sub> content is concerned, the formation of porosity is not hindered by the presence of TiO<sub>2</sub>. On the contrary, TiO<sub>2</sub> rather serves as a flux that can facilitate the reduction process and the development of porosity. Nevertheless, the main dynamics of porosity formation due to reduction seems to be consistent regardless of the TiO<sub>2</sub> content.

Various 2D sections were then selected to carry out simulations with the COMSOL Multiphysics software. The pellet with a composition of 0.0 % TiO<sub>2</sub> with mean diameter in top 2D direction is shown in Fig. 10. The corresponding binarized image created with IMAGEJ software is shown in Fig. 5S in the Supplementary Material and is available as online material.

The unreduced pellet picture is re-elaborated with ImageJ software, then simulation is performed as shown in Fig. 11.

A simulation is then carried out to follow the evolution of porosity over time, as shown in Fig. 12. The same simulation procedure was performed for medium sized pellets in different views. The corresponding analyses can be found in the supplementary material in Fig. 6S

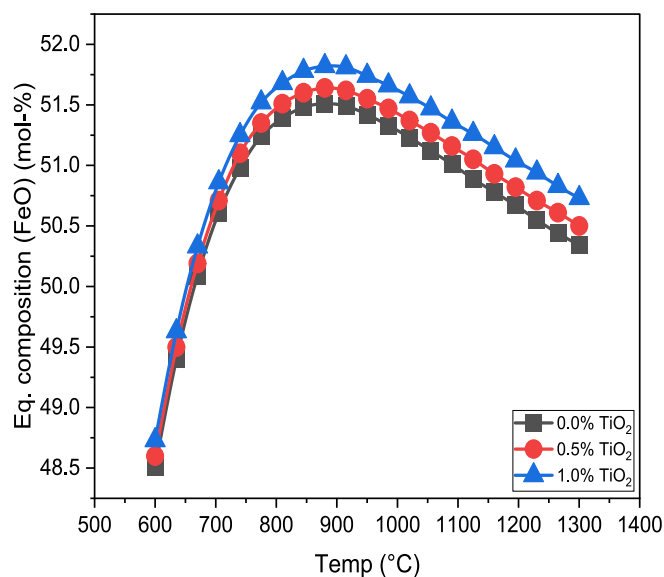


Fig. 5. Evolution of the equilibrium composition of FeO concentration for different pellets during HyDR as a function of temperature.

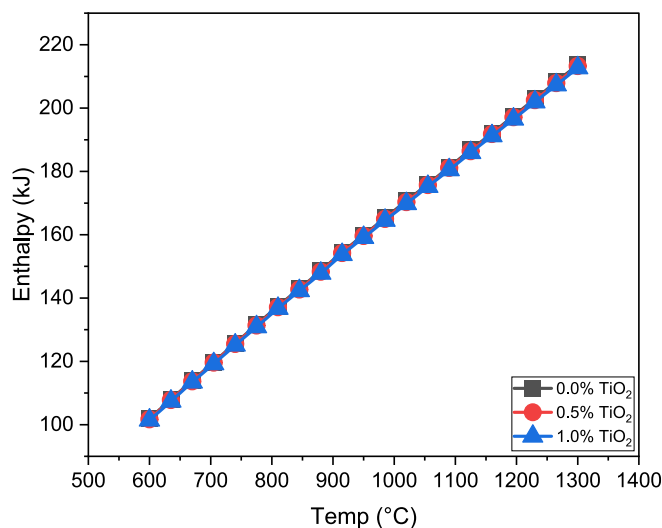


Fig. 6. The estimated enthalpy for the different composition of the pellets as function of temperature.

and Table 1S.

Fig. 12 shows a two-part visual analysis of porosity in a medium-sized pellet with a composition of 0.0 % TiO<sub>2</sub>. Fig. 12 (a) shows a series of contour plots depicting the evolution of porosity over time in the front view at intervals from 5 min to 50 min. Fig. 12 (b) shows a graph comparing the change in porosity over time from three different views. It is evident that porosity increases over time, with the greatest changes occurring in the early stages of the reduction process. This is indicated by the expansion of the contour lines, which represent areas of higher porosity. The contour density and rate of expansion appear to slow down over time, indicating a slowing of the porosity change after a period of time. Furthermore, Fig. 12 (b) quantifies this observation by showing the percentage change in porosity over time from the three views. All three curves follow a similar trend, with a rapid increase in porosity within the first 20 min, followed by a plateau effect as the response progresses. The right view shows slightly higher porosity values than the front and top views, which could indicate directional differences in the reduction process or inhomogeneities within the pellet. The trends in Fig. 6S, which also shows the reduction process and porosity variations over time, are consistent with the results in Fig. 12. This consistency between the figures and views confirms the reproducibility and reliability of the simulation results. The similarities in the trends of porosity evolution in Fig. 12 and Fig. 6S can be used to validate the COMSOL Multiphysics simulations for the reduction process. Hence, it can be deduced that the reduction kinetics and the associated increase in porosity are not only time-dependent, but also show a certain dependence on the spatial orientation within the pellet.

Furthermore, the same simulation procedure was followed for medium size pellets of different compositions. The corresponding analyses is shown in the supplementary material in Fig. 7S–9S and Tables 2S and 3S. It can be seen from Fig. 9S that the 0.0 % TiO<sub>2</sub> pellets show significant changes in porosity over time, with the areas of highest porosity increasing as time progresses, indicating an active reduction process. The 0.5 % TiO<sub>2</sub> pellets show slightly more gradual changes in porosity distribution. In the early stages, porosity is lower than in the 0.0 % TiO<sub>2</sub> pellets, but in the later stages, porosity also increases significantly. Finally, the 1.0 % TiO<sub>2</sub> pellets show a more localized increase in porosity, especially in the later periods, suggesting that higher TiO<sub>2</sub> concentrations may affect the uniformity and spread of the reduction process within the pellet. This comparative analysis shows how the TiO<sub>2</sub> concentration affects the porosity distribution and the kinetics of the reduction process in hematite pellets.

Fig. 13 shows a quantitative analysis of porosity variation in

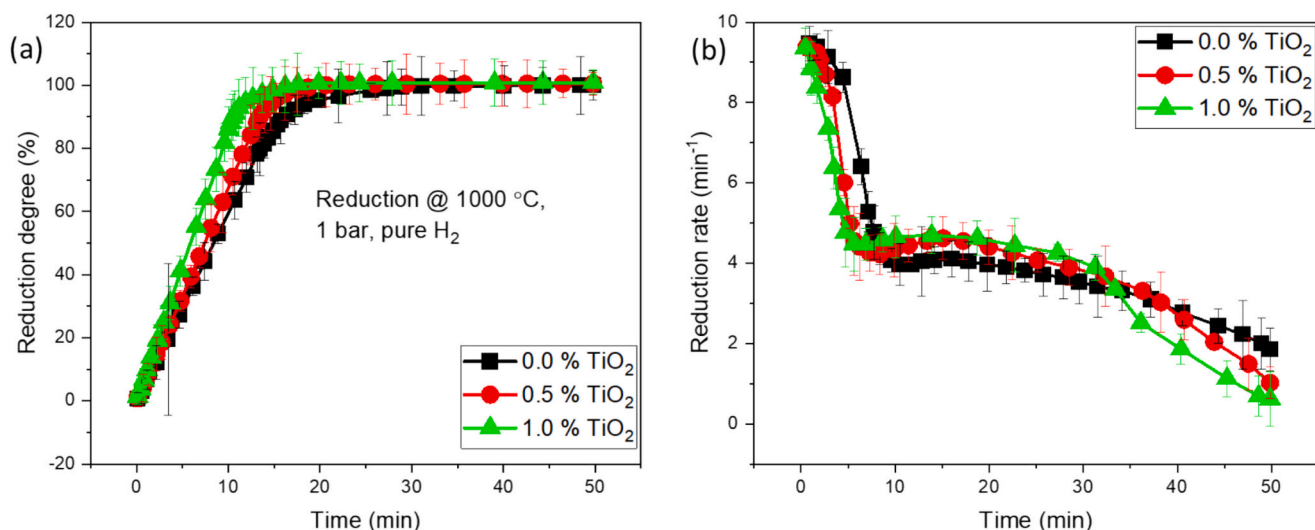


Fig. 7. Reduction kinetics of hematite pellets during HyDR for different pellet compositions with various  $TiO_2$  content at  $1000\text{ }^\circ\text{C}$ , (a) reduction degree, and (b) reduction rate, as function of time.

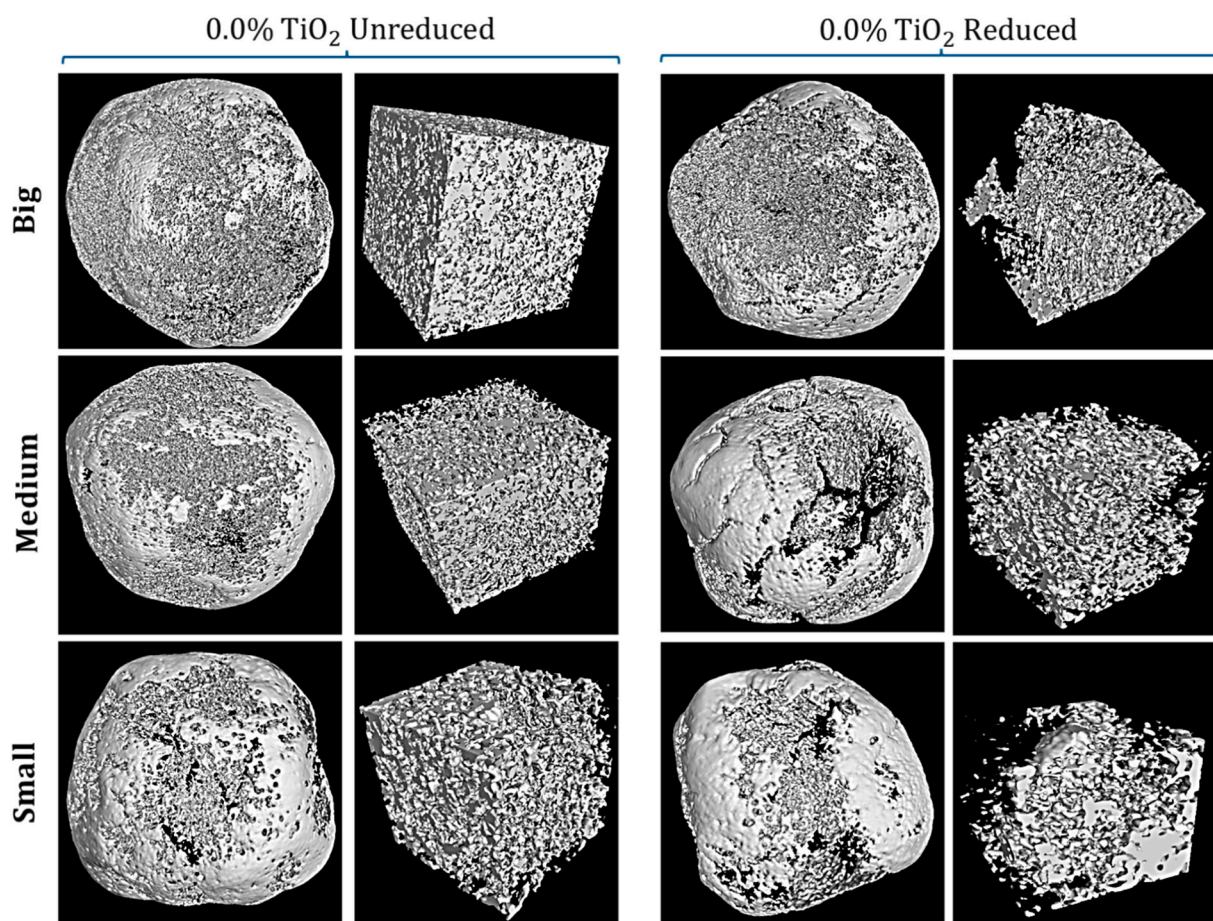
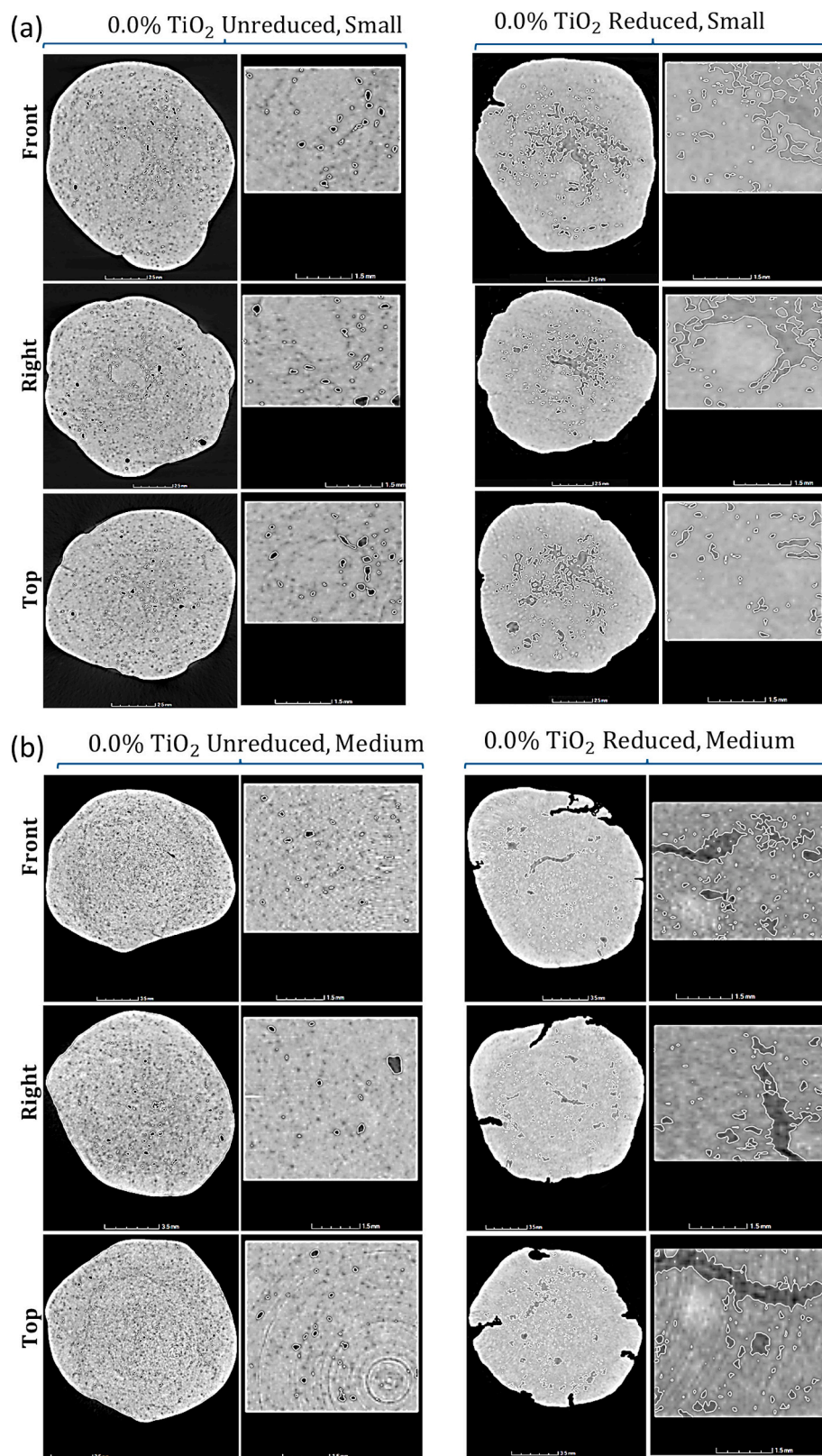


Fig. 8. 3D-microtomographic appearance of different sized pellets containing 0.0%  $TiO_2$  before and after HyDR at  $1000\text{ }^\circ\text{C}$  for 50 min.

medium-sized pellets with different  $TiO_2$  contents as a function of reduction time. For 0.0%  $TiO_2$  pellets, porosity increases sharply in the first 20 min, indicating a rapid reduction reaction. After this time, the increase in porosity slows down and levels off at a plateau, indicating that most of the reduction has taken place and the rate of change in porosity is decreasing. Furthermore, a similar pattern to the 0.0%  $TiO_2$  pellets is seen, but the overall porosity is slightly lower at each time

point. The initial rate of increase is comparable, but the peak porosity is not as high, which may indicate that the presence of  $TiO_2$  mitigates the reduction process to some extent. At the highest  $TiO_2$  content, namely 1.0%  $TiO_2$ , the clearest behavior is observed with a slightly slower initial increase in porosity. While the porosity still increases rapidly in the early phase, it does not reach the same level as for the 0.0%  $TiO_2$  pellets. The overall trend indicates that a higher  $TiO_2$  content has a



**Fig. 9.** 2D-microtomographic appearance of different sections of pellets containing 0.0 %TiO<sub>2</sub> before and after HyDR at 1000 °C for 50 min for different sized pellets, namely (a) small, (b) medium, and (c) big.

noticeable effect on the reduction process and the resulting porosity. In this regard, it should be noted that the contour plots for the 0.0 % TiO<sub>2</sub> pellets in Fig. 9S show extensive areas of high porosity, which is

consistent with the high percentage of porosity variation in Fig. 13. In addition, the 0.5 % TiO<sub>2</sub> pellets in Fig. 9S show a slightly more restrained evolution of porosity, which is also consistent with the

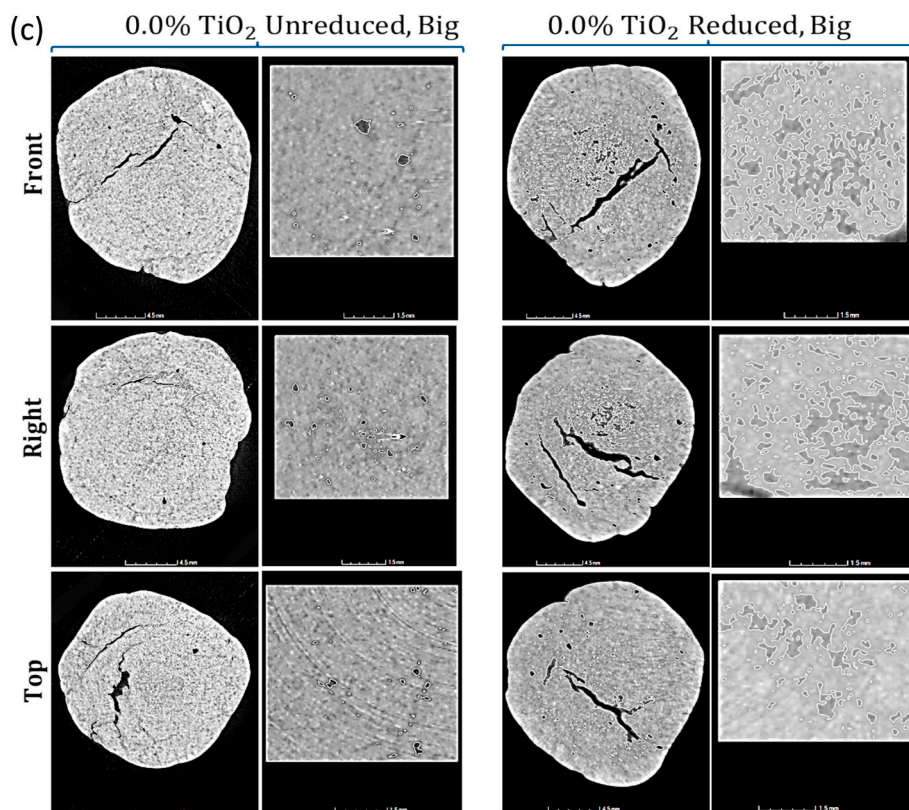


Fig. 9. (continued).

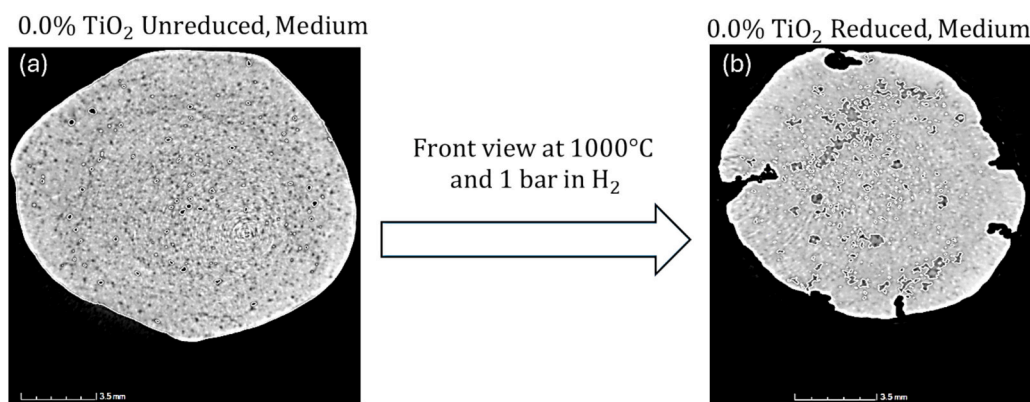


Fig. 10. Top View of  $\text{Fe}_2\text{O}_3$  Pellet Transformation. (a) Pre-reduction medium pellet with 0.0 %  $\text{TiO}_2$ . (b) Post-reduction at 1000 °C and 1 bar  $\text{H}_2$ , indicating porosity changes for COMSOL simulations.

slightly lower percentage of porosity variation in Fig. 13. Finally, for the 1.0 %  $\text{TiO}_2$  pellets, Fig. 9S shows localized areas of high porosity that correlate with the lower and more gradual increase in porosity in Fig. 13.

The last carried out analyses was about the potential of porosity different evolution under different  $\text{H}_2$  pressures during direct reduction. Fig. 14 shows the development of porosity in a big pellet with 0.0 %  $\text{TiO}_2$  content at 1000 °C under two different  $\text{H}_2$  pressures. The corresponding analyses of big pellets for different  $\text{TiO}_2$  content at 8 bar  $\text{H}_2$  pressure is shown in the supplementary material in Fig. 10S- 15S and Table 4S and 5S. The comparison of Fig. 14 with Fig. 12S shows a similar pattern of porosity evolution for the 0.0 %  $\text{TiO}_2$  pellets. The porosity is initially concentrated in the center and then spreads outward with time. The pattern is the same in both figures, which shows the reproducibility of the reduction process at 1 bar  $\text{H}_2$  pressure. Similarly, the pellets reduced

at 8 bar  $\text{H}_2$  pressure show a faster and more uniform development of porosity in both figures than the pellets reduced at 1 bar. The higher pressure enables faster reaction kinetics and a more homogeneous distribution of porosity, independent of the  $\text{TiO}_2$  content.

Fig. 15 shows a graphical representation of the change in porosity as a function of reduction time for a big pellet at 1000 °C under different  $\text{H}_2$  pressures and with different  $\text{TiO}_2$  contents. At a pressure of 1 bar, the porosity of the 0.0 %  $\text{TiO}_2$  pellet increases steadily until about 30 min and then levels off. At a pressure of 8 bar, the porosity increases faster and reaches higher values before reaching a plateau. This shows that a higher pressure accelerates the reduction process and leads to greater porosity. For 0.5 %  $\text{TiO}_2$  pellets, a faster and higher increase in porosity is observed at 8 bar compared to 1 bar. The trend is similar to the 0.0 %  $\text{TiO}_2$  pellet, with 8 bar pressure leading to a faster and greater increase in porosity. The presence of  $\text{TiO}_2$  does not change the fact that higher

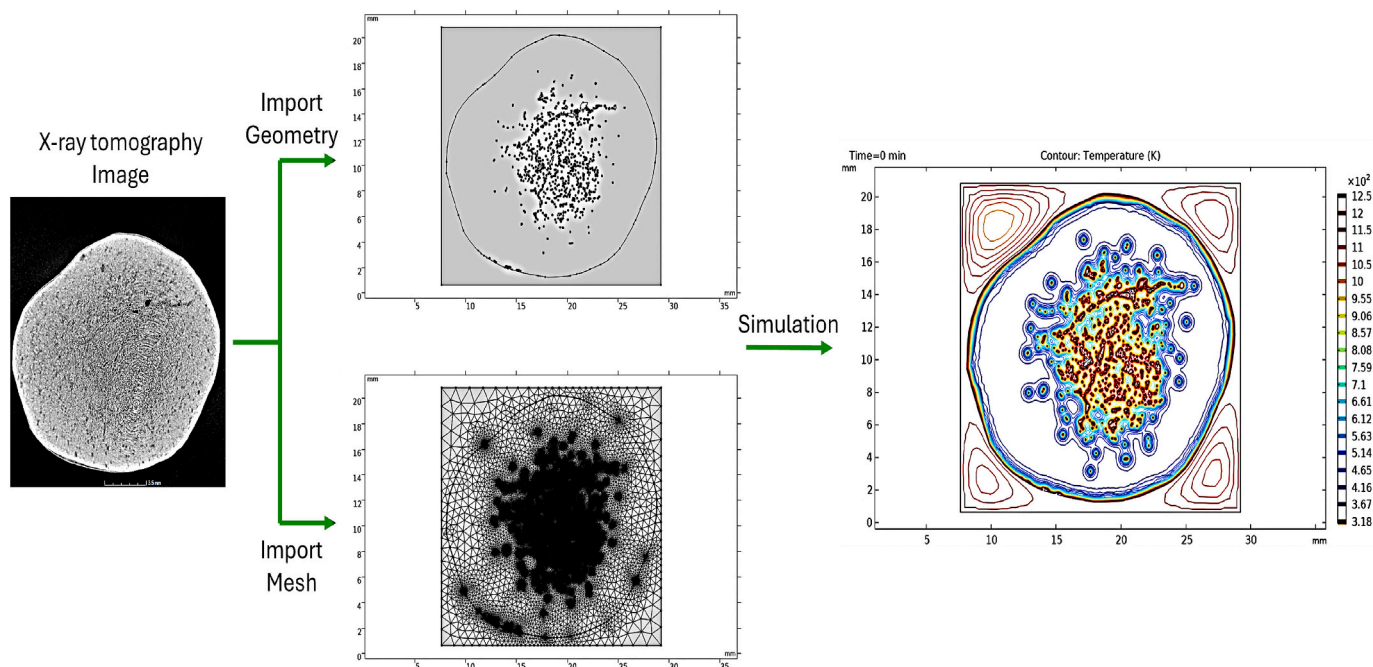
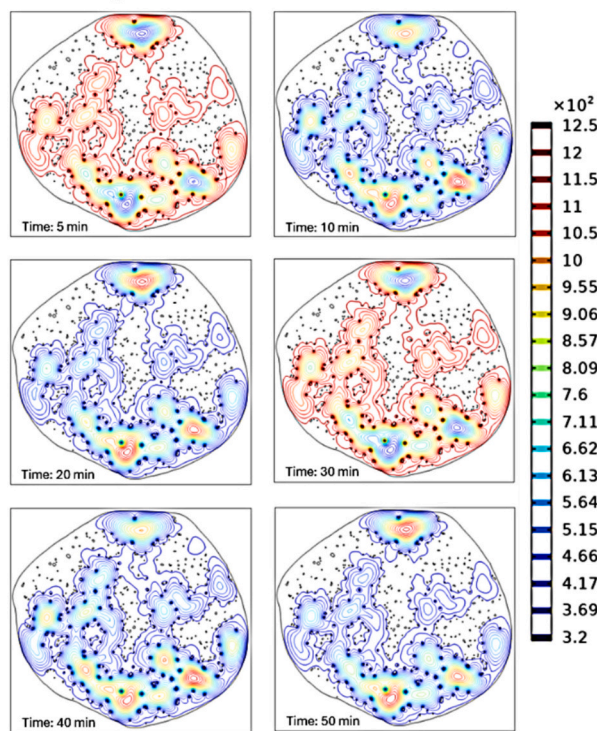


Fig. 11. Initial simulation steps for front view of the medium pellets reduced at 1000 °C and H<sub>2</sub>.

### Porosity evolution



### Porosity variation

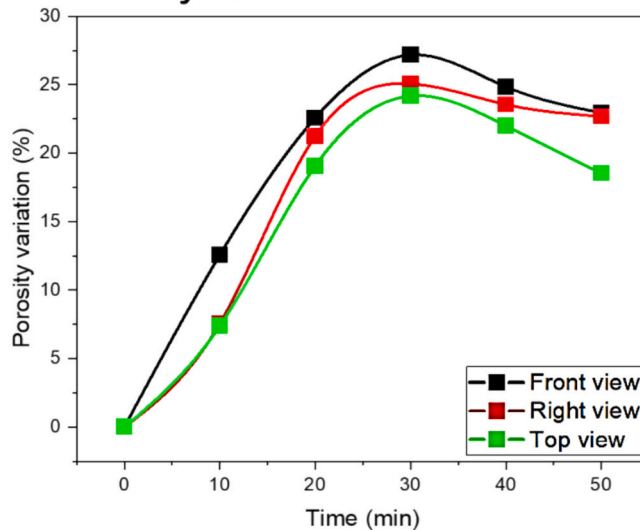


Fig. 12. Porosity comparison for front view of medium-sized pellet 0.0 % TiO<sub>2</sub> reduced at 1000 °C and H<sub>2</sub> (a) Porosity evolution, and (b) The quantified Porosity variation in three views.

pressure improves the reduction process. Again, the curve for 8 bar pressure shows a faster increase in porosity of the 1.0 % TiO<sub>2</sub> pellet compared to 1 bar pressure. The pellet with a higher TiO<sub>2</sub> content still benefits from the higher pressure and shows a steep increase in porosity, exceeding the porosity achieved at 1 bar pressure. It is clear how an increase in H<sub>2</sub> pressure leads to an increase in porosity (Fig. 15). The results of simulations in different TiO<sub>2</sub> content are shown in Fig. 16. It is

also obvious that as TiO<sub>2</sub> increases, the porosity variation increases. The same analyses was performed for big pellets with 0.5 and 1.0 % TiO<sub>2</sub>, the images reconstructions and the simulations results are shown in Supplementary material.

The enthalpy increasing with temperature indicates a lower thermodynamic favourability, meaning that higher temperatures could potentially hinder the reaction due to the greater energy demand. The

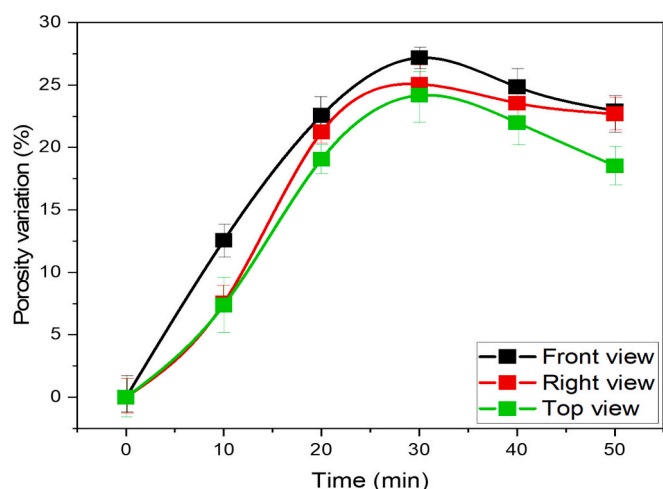


Fig. 13. The quantified Porosity variation of medium size pellets with different  $\text{TiO}_2$  content reduced at  $1000\text{ }^\circ\text{C}$  and  $\text{H}_2$  as function of reducing time.

occurrence of numerous cracks with increasing  $\text{TiO}_2$  content can be attributed to the coalescence of the pores. In fact, as the  $\text{TiO}_2$  content increases, the structural changes during reduction also increase. From the differences in the reduction rates shown in Fig. 7, it can be seen that the reduction rate during the first intermediate stage of reduction, namely hematite to magnetite, by  $\text{TiO}_2$  decreases significantly over time. This can be explained by the fact that the presence of  $\text{TiO}_2$  tends to hinder the chemical reactions, which in turn has an effect on the overall

reduction process. Due to the specific crystal structure of  $\text{TiO}_2$  (tetragonal) and other compounds such as  $\text{CaTiO}_3$  [13] (orthorhombic), the phenomenon of active diffusion is limited. During the hydrogen-based direct reduction process,  $\text{TiO}_2$  can be partially reduced or interact with the surrounding phases, leading to the formation of complex compounds such as  $\text{CaTiO}_3$ . This reaction limits the reducibility of the pellets due to the stable nature of these titanium-containing phases. More precisely, due to the complex crystal structure of these compounds, the activation energy of effective diffusion increases and, on the other hand, it becomes more difficult. In this sense, Paananen et al. [11] found that the higher the  $\text{TiO}_2$  content of the hematite, the more fragmented and dissolved the reduction front. Additionally,  $\text{TiO}_2$  contributes to changes in porosity and diffusion pathways within the pellet by affecting gas-solid interactions and microstructural transformations. The stabilization of certain lattice structures by  $\text{TiO}_2$  slows down oxygen removal, making the reduction kinetics less favorable at higher  $\text{TiO}_2$  concentrations. As a result, the reducibility of the iron oxide pellets is reduced. Despite the thermodynamic implications, the kinetic effects of temperature on reaction rates are significant. At higher temperatures, the molecules have higher kinetic energy, increasing the frequency of effective collisions and making it easier to overcome the activation energy barrier. This aspect underlines how important it is to consider both thermodynamics and kinetics when evaluating reaction progress. Because even if a reaction is thermodynamically less favorable at high temperatures, the improved kinetics could still drive the reaction forward.

Noting this point is necessary that experimental scatter, represented by the standard deviation of reduction rates, was within  $\pm 2\text{--}4\%$  for all conditions tested. This variability indicates consistent experimental results, with smaller variations due to intrinsic factors such as temperature

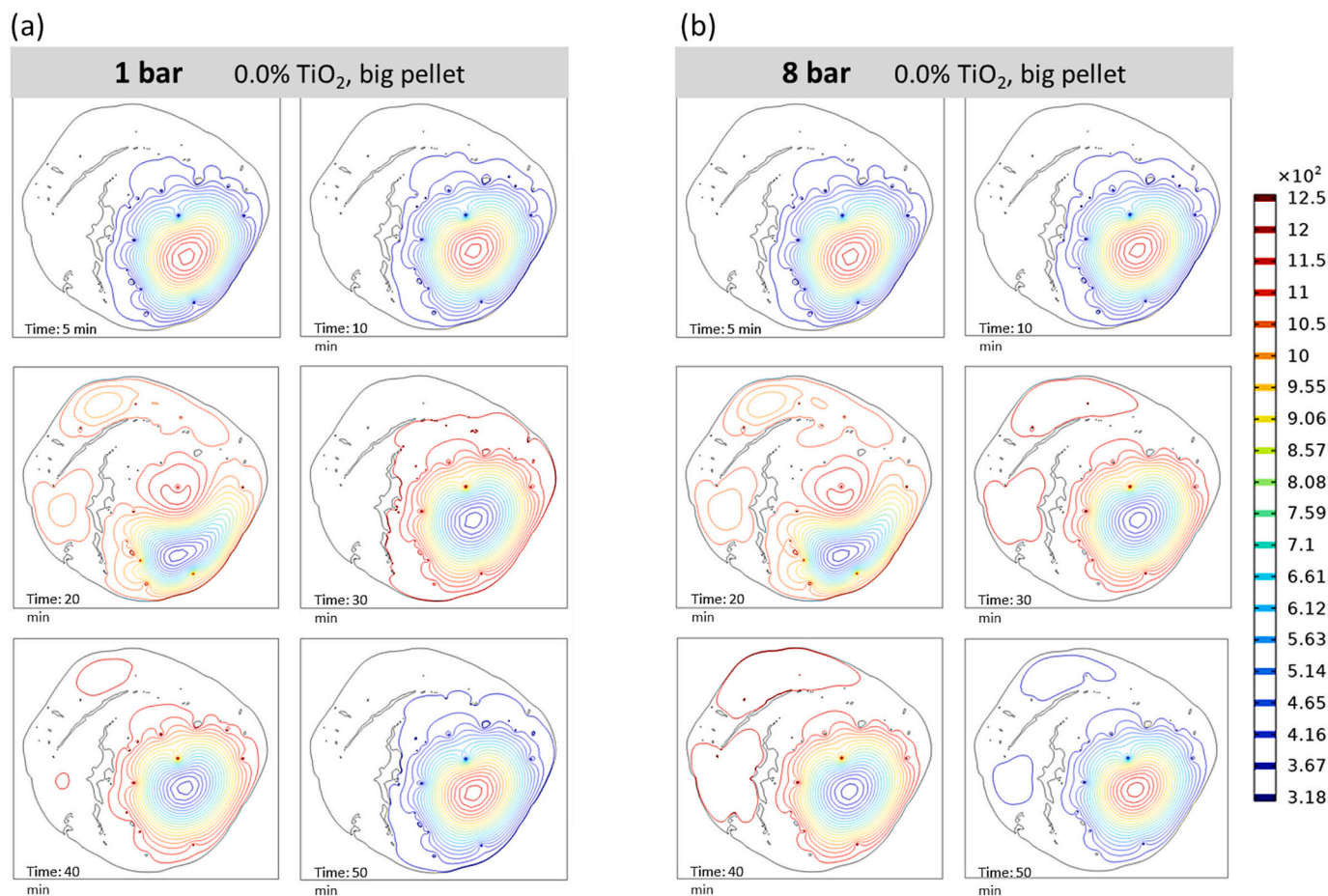


Fig. 14. Porosity evolution for top view of the big pellet with  $0.0\%$   $\text{TiO}_2$  reduced at  $1000\text{ }^\circ\text{C}$  and different  $\text{H}_2$  pressure, (a) 1 bar, and (b) 8 bar.



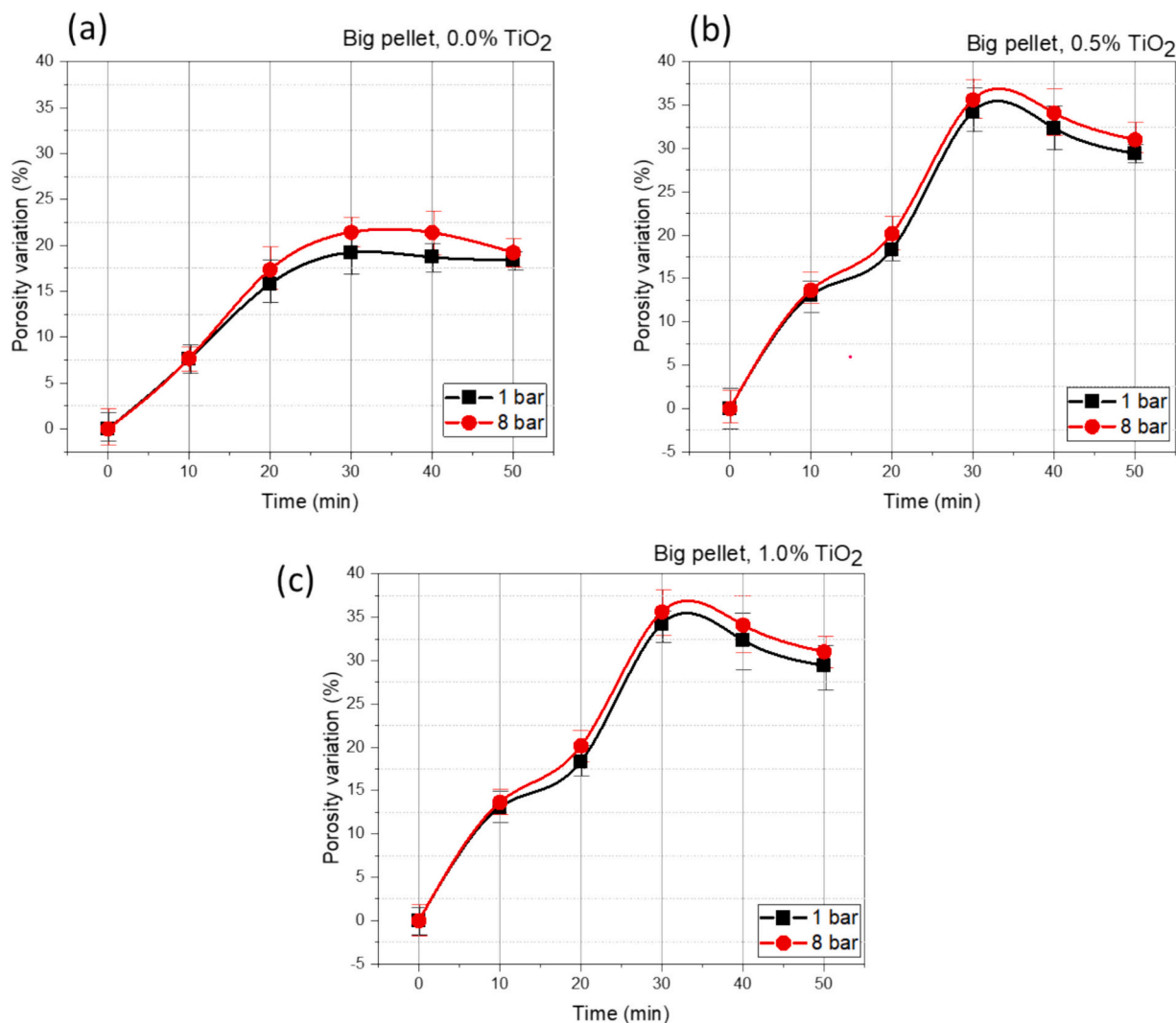


Fig. 15.  $H_2$  pressure dependent quantified porosity variation as function of reducing time for big pellet with different  $TiO_2$  content reduced at 1000 °C.

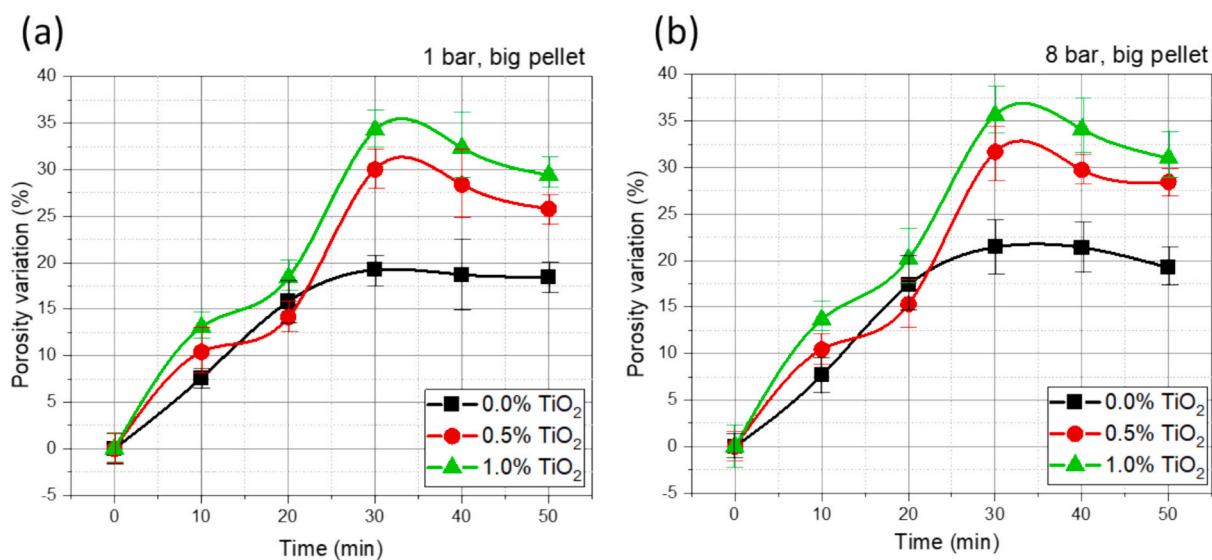


Fig. 16. The quantified porosity variation as function of reducing time in big pellet with different  $TiO_2$  content in  $H_2$  pressure of (a) 1 bar, and (b) 8 bar.

**Table 4**  
Impact of TiO<sub>2</sub> Content on the Reducibility of Iron Ore Pellets Under Different Hydrogen Pressures.

TiO <sub>2</sub> Content (%)	Porosity Increase at 1 bar (%)	Porosity Increase at 8 bar (%)	Reduction Degree at 1 bar (%)	Reduction Degree at 8 bar (%)	Structural Integrity	Reaction Kinetics
0.0	15	25	90	97	High	Rapid
0.5	12	22	87	95	Moderately high	Moderately rapid
1.0	8	18	80	89	Moderate	Moderate

stability and gas flow uniformity. When comparing the significance of this scatter with the influence of TiO<sub>2</sub> content on reduction kinetics, it is found that although there is inherent experimental variability, the effects of TiO<sub>2</sub> are more pronounced. For example, pellets with 0.0 % TiO<sub>2</sub> exhibited a higher rate of reduction and a higher degree of porosity change than those with 0.5 % and 1.0 % TiO<sub>2</sub>. The variability of the reduction kinetics due to TiO<sub>2</sub> content exceeded the standard deviation, confirming that the influence of TiO<sub>2</sub> was significant compared to the experimental scatter. The experimental scatter thus underlines the robustness of the observed results and shows that the trends linked to TiO<sub>2</sub> content were not obscured by experimental noise but were a clear consequence of compositional differences.

TiO<sub>2</sub> plays a complex role in the reducibility of iron ore pellets. On the one hand, the presence of TiO<sub>2</sub> in small amounts could potentially act as a catalyst and improve the reduction process at the beginning due to its effects on the microstructure of the pellet. This could be due to the formation of microcracks and voids within the pellet, which can increase the surface area available for the reduction reaction and facilitate the diffusion of H<sub>2</sub>. However, if the TiO<sub>2</sub> content rises above a critical threshold (especially above 0.5 wt%), this has a detrimental effect on the reducibility. The presence of higher TiO<sub>2</sub> contents correlate with a decrease in porosity, which is a key factor for the reduction process as it influences the gas flow within the pellet. Moreover, CaTiO<sub>3</sub> is likely to form around hematite [13], where it hinders hematite bonding, leading to a decrease in surface reactions and consequently a disruption in the reducibility of the pellet. Lower porosity hinders the diffusion of the reducing gasses and thus reduces the overall rate of the reduction reaction. In addition, TiO<sub>2</sub> can lead to the formation of stable oxides that are more difficult to reduce, and it can contribute to the reoxidation of the already reduced iron, especially when the pellets are exposed to oxidizing conditions after reduction. The addition of TiO<sub>2</sub> in excess of 0.5 % by weight has also been associated with an increase in reduction-induced degradation, such as cracking, which can have a negative impact on the mechanical integrity of the pellets.

During HyDR process, iron oxides are reduced to metallic Fe by the removal of oxygen atoms. This reduction involves the conversion of Fe<sup>+3</sup> ions into Fe<sup>+2</sup> ions [29–32]. When oxygen is removed, the Fe<sup>+3</sup> ions lose an oxygen atom and transform into Fe<sup>+2</sup> ions [33]. This transformation increases the concentration of Fe<sup>+2</sup> ions in the lattice structure of the pellet. It is important to note that the increased concentration of Fe<sup>+2</sup> ions in the lattice accelerates the reduction process of Fe<sup>+2</sup> to metallic iron. The more Fe<sup>+2</sup> ions present, the more places there are for H<sub>2</sub> atoms (from the H<sub>2</sub> gas) to react with, resulting in faster reduction to metallic iron. Conversely, the increase in the Fe<sup>+2</sup> concentration also slows down the reduction of Fe<sup>+3</sup> ions to Fe<sup>+2</sup> ions. This is because if fewer Fe<sup>+3</sup> ions are available due to their reduction to Fe<sup>+2</sup>, there are also fewer Fe<sup>+3</sup> sites where oxygen removal can take place. In addition, the Ti<sup>+4</sup> ions of TiO<sub>2</sub> contribute to the stabilization of the lattice structure by forming strong bonds with oxygen atoms. The Ti<sup>+4</sup> ions have a stable configuration with six oxygen atoms in an octahedral environment. This stable configuration acts as a stabilizing factor that makes it difficult for oxygen to be removed from the lattice during the reduction process. As a result, the presence of Ti<sup>+4</sup> ions further slows down the removal of oxygen, contributing to the slowing down of the overall reduction process. As a result, the removal of oxygen atoms from

Fe<sub>2</sub>O<sub>3</sub> is made more difficult by the presence of TiO<sub>2</sub>, which acts as a stabilizing factor. The presence of TiO<sub>2</sub> leads to a more controlled reduction process with a gradual conversion of Fe<sup>+3</sup> to Fe<sup>+2</sup> and the subsequent formation of metallic Fe.

The operating pressure during the reduction process has a considerable influence on the effect of TiO<sub>2</sub> on reducibility [34]. At higher pressure, the availability of H<sub>2</sub> increases, which can increase the reduction rate and lead to a more uniform and extensive development of porosity within the pellet. This is particularly beneficial for pellets with a higher TiO<sub>2</sub> content, as the increased pressure can partially offset the negative effects of TiO<sub>2</sub> on porosity and reducibility. In addition, porosity, pore size and tortuosity have a significant impact on entropy changes during the reduction steps [35,36], with entropy generation starting early due to heat transfer between gas and pellets. Thus, when the H<sub>2</sub> pressure increases, the resistance of the pellets to the diffusion of the gas decreases thanks to the higher accessibility of the H<sub>2</sub> atoms. As a result, the rate of entropy generation decreases and the reduction effect is enhanced. While TiO<sub>2</sub> influences the reduction process both at a pressure of 1 bar and at 8 bar, increasing the pressure tends to weaken the localizing effects of TiO<sub>2</sub> on the porosity distribution. The high pressure superimposes the influence of TiO<sub>2</sub> and leads to a more uniform porosity of the pellets, even at higher TiO<sub>2</sub> concentrations. This suggests that the operating pressure may be a crucial parameter to mitigate the adverse effects of higher TiO<sub>2</sub> concentrations and improve the overall reducibility of the pellets. It can be concluded that the percentage of TiO<sub>2</sub> in high-quality iron ore pellets and the pressure in the reduction process are crucial variables that influence the direct reducibility of the material. While low TiO<sub>2</sub> contents can have a positive effect on the reduction process, especially under high pressure conditions, higher concentrations lead to reducibility problems, possibly due to reduced porosity and stabilization of non-reducible oxides.

Table 4 provides important quantitative insights into the effects of TiO<sub>2</sub> content on the reducibility of iron ore pellets at different hydrogen pressures. As observed, there is a clear trend where increasing TiO<sub>2</sub> content consistently correlates with lower porosity and lower reducibility. For example, pellets with a TiO<sub>2</sub> content of 0.0 % show a significant increase in porosity (15 % at 1 bar and 25 % at 8 bar) and a high degree of reduction (90 % at 1 bar and 97 % at 8 bar). This indicates that lower TiO<sub>2</sub> contents improve the microstructural properties of the pellets, allowing greater diffusion of hydrogen and more effective reduction reactions. On the other hand, when the TiO<sub>2</sub> content increases to 1.0 %, there is a significant decrease in porosity and the degree of reduction at both pressure conditions. The increase in porosity decreases to 5 % at 1 bar and 15 % at 8 bar, with the degree of reduction also decreasing to 80 % and 89 % respectively. This decrease in porosity and degree of reduction at higher TiO<sub>2</sub> contents can be attributed to the formation of more stable and complex oxides, which are more difficult to reduce. In addition, the structural integrity of the pellets decreases with higher TiO<sub>2</sub> contents, suggesting that excessive TiO<sub>2</sub> content leads to a compromised pellet structure, potentially resulting in mechanical weaknesses that could affect their handling and use in reduction furnaces. The reaction kinetics also show a slowing trend with increasing TiO<sub>2</sub> content, suggesting that the presence of TiO<sub>2</sub> complicates the chemical reactions required for efficient reduction. However, increasing the hydrogen pressure from 1 bar to 8 bar tends to mitigate these negative effects and increases both the porosity and the degree of

reduction at all TiO<sub>2</sub> contents. This improvement under higher pressure conditions suggests that operational adjustments, such as increasing the hydrogen pressure, can partially counteract the detrimental effects of high TiO<sub>2</sub> concentrations and improve the overall efficiency of the reduction process. This underscores the importance of carefully controlling TiO<sub>2</sub> content and operating parameters to maximize direct reducibility and mechanical quality of the pellets.

#### 4. Conclusion

In summary, the direct reducibility of high-grade iron ore pellets at 1000 °C under 1 and 8 bar H<sub>2</sub> pressure is significantly affected by the percentage of TiO<sub>2</sub> and the operating pressure during the reduction process.

1. The study shows that lower concentrations of TiO<sub>2</sub> improve the reduction process, with an increase in porosity and reduction rate being observed. In particular, pellets with 0.0 % TiO<sub>2</sub> showed a faster initial increase in porosity compared to those with higher TiO<sub>2</sub> concentrations. In contrast, pellets with TiO<sub>2</sub> concentrations above 0.5 % exhibited lower porosity and slower reduction rates. Thus, the porosity in pellets with 1.0 % TiO<sub>2</sub> was consistently lower at different stages of the reduction process, with the porosity expansion rate decreasing significantly after the first 20 min of reduction.
2. The reaction kinetics improved with increasing temperature, as higher temperatures facilitated the reduction of Fe<sub>2</sub>O<sub>3</sub> to Fe<sub>3</sub>O<sub>4</sub> and then to Fe. However, the presence of TiO<sub>2</sub> increased the thermodynamic energy requirement, especially at temperatures above 950 °C, where the reduction efficiency of pellets with higher TiO<sub>2</sub> content was significantly less favorable. At 1000 °C, for example, the reduction rate for pellets with 0.0 % TiO<sub>2</sub> was significantly higher than that for pellets with 1.0 % TiO<sub>2</sub>.
3. Increased H<sub>2</sub> pressure significantly improved the reducibility of the pellets. At 1 bar, the porosity of pellets with 0.0 % TiO<sub>2</sub> increased by about 15 % within 50 min, while at 8 bar it increased by almost 25 % within the same time span. This emphasizes the role of pressure in offsetting the negative effects of higher TiO<sub>2</sub> concentrations and promotes a more uniform and extensive porosity development in all tested pellets.
4. The structural integrity and porosity of the pellets were significantly affected by TiO<sub>2</sub> content. High-resolution tomography showed a more pronounced development of microcracks in pellets with higher TiO<sub>2</sub> contents, especially at values above 0.5 %. These structural changes were associated with a more fragmented reduction front, which had a negative impact on the mechanical properties and reducibility of the pellets.
5. The agreement between the COMSOL Multiphysics simulation results and the experimental data was robust and showed consistent trends in porosity evolution and reduction kinetics. For example, the simulations predicted a 20 % increase in porosity for 0.0 % TiO<sub>2</sub> pellets at 1000 °C, which exactly matched the experimental increase of 18–22 % observed under similar conditions.

For optimal performance in steelmaking, it is recommended to keep the TiO<sub>2</sub> content at or below 0.5 %. Adjustments to the reduction conditions, such as increasing the H<sub>2</sub> pressure to 8 bar, can significantly improve the reducibility and quality of the pellets, especially those with higher TiO<sub>2</sub> concentrations. This approach not only improves reduction efficiency, but also ensures the structural integrity of the pellets, which is essential for their subsequent use in steel production.

#### CRedit authorship contribution statement

**Behzad Sadeghi:** Writing – review & editing, Writing – original draft, Visualization, Validation, Supervision, Resources, Project administration, Methodology, Investigation, Formal analysis, Data curation,

Conceptualization. **Pasquale Cavaliere:** Writing – review & editing, Validation, Supervision, Software, Resources, Methodology, Investigation, Funding acquisition. **Mutlucan Bayat:** Software, Formal analysis, Conceptualization. **Marieh Aminaei:** Software, Conceptualization. **Niloofer Ebrahimzadeh Esfahani:** Writing – original draft, Software, Methodology, Investigation, Data curation, Conceptualization. **Aleksandra Laska:** Visualization, Methodology, Formal analysis. **Damian Koszelow:** Visualization, Methodology, Formal analysis. **Natalia Ramos Goncalves:** Software, Conceptualization.

#### Declaration of competing interest

The authors declare the following financial interests/personal relationships which may be considered as potential competing interests.

Pasquale cavaliere reports financial support was provided by University of Salento Department of Engineering Innovation. Pasquale cavaliere reports a relationship with University of Salento Department of Engineering Innovation that includes: employment. If there are other authors, they declare that they have no known competing financial interests or personal relationships that could have appeared to influence the work reported in this paper.

#### Acknowledgments

The authors would like to thank the Italian Ministry for University and Research (MUR) for the fundings provided under the Grant “green hydrogen for clean steels, kinetics and modeling in the direct reduction of iron oxides, decarbonization of hard to abate industry– “real-green-steels”, P202278BNF.

#### Data availability

Data will be made available on request.

#### References

- [1] D. Raabe, M. Jovičević-Klug, D. Ponge, A. Gramlich, A.K. da Silva, A.N. Grundy, et al., Circular steel for fast Decarbonization: thermodynamics, kinetics, and microstructure behind upcycling scrap into high-performance sheet steel, *Annu. Rev. Mater. Res.* 54 (2024).
- [2] D. Raabe, C.C. Tasan, E.A. Olivetti, Strategies for improving the sustainability of structural metals, *Nature* 575 (2019) 64–74.
- [3] D. Raabe, The materials science behind sustainable metals and alloys, *Chem. Rev.* 123 (2023) 2436–2608.
- [4] E.G. Hertwich, S. Ali, L. Ciacci, T. Fishman, N. Heeren, E. Masanet, et al., Material efficiency strategies to reducing greenhouse gas emissions associated with buildings, vehicles, and electronics—a review, *Environ. Res. Lett.* 14 (2019) 043004.
- [5] I.R. Souza Filho, H. Springer, Y. Ma, A. Mahajan, C.C. da Silva, M. Kulse, et al., Green steel at its crossroads: hybrid H<sub>2</sub>-based reduction of iron ores, *J. Clean. Prod.* 340 (2022) 130805.
- [6] L. Choisez, K. Hemke, Ö. Özgün, C. Pistidda, H. Jeppesen, D. Raabe, et al., H<sub>2</sub>-based direct reduction of combusted iron powder: deep pre-oxidation, reduction kinetics and microstructural analysis, *Acta Mater.* 268 (2024) 119752.
- [7] Y. Ma, I.R. Souza Filho, Y. Bai, J. Schenk, F. Patisson, A. Beck, et al., Hierarchical nature of H<sub>2</sub>-based direct reduction of iron oxides, *Scr. Mater.* 213 (2022) 114571.
- [8] V. Vogl, M. Åhman, L.J. Nilsson, Assessment of H<sub>2</sub> direct reduction for fossil-free steelmaking, *J. Clean. Prod.* 203 (2018) 736–745.
- [9] F. Rosner, D.D. Papadias, K.P. Brooks, K.O. Yoro, R.K. Ahluwalia, T.S. Autrey, et al., Green steel: design and cost analysis of H<sub>2</sub>-based direct iron reduction, *Energy Environ. Sci.* 16 (2023) 4121–4134.
- [10] T. Paananen, The Effect of Minor Oxide Components on Reduction of iron Ore Agglomerates: Verlag Nicht Ermitteltbar, 2013.
- [11] T. Paananen, K. Kinnunen, Effect of TiO<sub>2</sub>-content on reduction of iron ore agglomerates, *Steel Res. Int.* 80 (2009) 408–414.
- [12] H. Pimenta, V. Seshadri, Influence of Al<sub>2</sub>O<sub>3</sub> and TiO<sub>2</sub> degradation behaviour of sinter and hematite at low temperatures on reduction, *Ironmak. Steelmak.* 29 (2002) 175–179.
- [13] J.T. Ju, Q.-d. Li, X. Xing, X. Jiang, G.-q. Zhao, F. Lu, Effect of high basicity on compressive strength and microstructure of iron ore pellets containing TiO<sub>2</sub>, *Metallurg. Res. & Technol.* 120 (2023) 306.
- [14] S. Yang, W. Tang, X. Xue, Effect of TiO(2) on the Sintering Behavior of Low-Grade Vanadiferous Titanomagnetite Ore, *Materials (Basel, Switzerland)* (2021) 14.
- [15] R. Prasad, S. Soren, L.A. Kumaraswamidhas, C. Pandey, S.K. Pan, Experimental Investigation of Different Fineness and Firing Temperatures on Pellets Properties of

- Different Iron Ore Fines from Indian Mines, *Materials* (Basel, Switzerland) (2022) 15.
- [16] P. Cavaliere, L. Dijon, A. Laska, D. Koszelow, H<sub>2</sub> direct reduction and reoxidation behaviour of high-grade pellets, *Int. J. H2 Energy*. 49 (2023) 1235–1254.
- [17] M. Auinger, D. Vogel, A. Vogel, M. Spiegel, M. Rohwerder, A novel laboratory set-up for investigating surface and interface reactions during short term annealing cycles at high temperatures, *Rev. Sci. Instrum.* 84 (2013).
- [18] P. Cavaliere, A. Perrone, L. Dijon, A. Laska, D. Koszelow, Direct reduction of pellets through H<sub>2</sub>: Experimental and model behaviour, *Int. J. H2 Energy*. 49 (2023) 1444–1460.
- [19] D. Spreitzer, J. Schenk, Reduction of iron oxides with H<sub>2</sub>—a review, *Steel Res. Int.* 90 (2019) 1900108.
- [20] K. Ma, J. Deng, G. Wang, Q. Zhou, J. Xu, Utilization and impacts of H<sub>2</sub> in the ironmaking processes: a review from lab-scale basics to industrial practices, *Int. J. H2 Energy*. 46 (2021) 26646–26664.
- [21] A. Heidari, N. Niknahad, M. Iljana, T. Fabritius, Review on the kinetics of Iron ore reduction by H<sub>2</sub>, *Materials* 14 (2021) 7540 (s Note: MDPI stays neutral with regard to jurisdictional claims in published ...; 2021).
- [22] A.A. Barde, J.F. Klausner, R. Mei, Solid state reaction kinetics of iron oxide reduction using H<sub>2</sub> as a reducing agent, *Int. J. H2 Energy*. 41 (2016) 10103–10119.
- [23] B. Hou, H. Zhang, H. Li, Q. Zhu, Study on kinetics of iron oxide reduction by H<sub>2</sub>, *Chin. J. Chem. Eng.* 20 (2012) 10–17.
- [24] A. Pineau, N. Kanari, I. Gaballah, Kinetics of reduction of iron oxides by H<sub>2</sub>: Part II. Low temperature reduction of magnetite, *Thermochim. Acta* 456 (2007) 75–88.
- [25] A. Pineau, N. Kanari, I. Gaballah, Kinetics of reduction of iron oxides by H<sub>2</sub>. Part I: Low temperature reduction of hematite, *Thermochim. Acta* 447 (2006) 89–100.
- [26] P. Cavaliere, H<sub>2</sub> Assisted Direct Reduction of iron Oxides, Springer, 2022.
- [27] -Y. Ma, -I.R.S. Filho, -X. Zhang, -S. Nandy, -P. Barriobero-Vila, -G. Requena, et al., H<sub>2</sub>-based direct reduction of iron oxide at 700°C: Heterogeneity at pellet and microstructure scales, *Int. J. Miner. Metall. Mater.* 29 (2022) 1901.
- [28] X. Zheng, S. Paul, L. Moghimi, Y. Wang, R.A. Vilá, F. Zhang, et al., Correlating Chemical Reaction and Mass Transport in H<sub>2</sub>-based Direct Reduction of Iron Oxide, *Proceedings of the National Academy of Sciences* 120 (2023) e2305097120.
- [29] B. Sadeghi, P. Cavaliere, M. Bayat, N. Ebrahimzadeh Esfahani, A. Laska, D. Koszelow, Experimental study and numerical simulation on porosity dependent direct reducibility of high-grade iron oxide pellets in hydrogen, *Int. J. Hydrog. Energy* 69 (2024) 586–607.
- [30] H.-y. Lin, Y.W. Chen, C. Li, The mechanism of reduction of iron oxide by H<sub>2</sub>, *Thermochim. Acta* 400 (2003) 61–67.
- [31] E. Park, O. Ostrovski, Reduction of titania-ferrous ore by carbon monoxide, *ISIJ Int.* 43 (2003) 1316–1325.
- [32] A.N. Dmitriev, R.V. Alektorov, G.Y. Vitkina, S.A. Petrova, Y.A. Chesnokov, Features of the reducibility of Titanomagnetite Iron ore materials, *Defect Diffus. Forum.* 400 (2020) 176–185.
- [33] S. Bonanni, K. Ait-Mansour, W. Harbich, H. Brune, Effect of the TiO<sub>2</sub> reduction state on the catalytic CO oxidation on deposited size-selected Pt clusters, *J. Am. Chem. Soc.* 134 (2012) 3445–3450.
- [34] P. Cavaliere, B. Sadeghi, A. Laska, D. Koszelow, TiO<sub>2</sub> and reducing gas: intricate relationships to direct reduction of Iron oxide pellets, *Metall. Mater. Trans. B Process Metall. Mater. Process. Sci.* 55 (5) (2024) 3431–3450.
- [35] P. Cavaliere, A. Perrone, D. Marsano, Effect of reducing atmosphere on the direct reduction of iron oxides pellets, *Powder Technol.* 426 (2023) 118650.
- [36] B. Sadeghi, M. Najafzadeh, P. Cavaliere, A. Shabani, M. Aminaei, Effect of composition and processing conditions on the direct reduction of iron oxide pellets, *Powder Technol.* 444 (2024) 120061.